Materials Science

Volume 2, Issue 3, 243-259.
DOI: 10.3934/matersci.2015.3.243
Received date 23 April 2015,
Accepted date 11 August 2015,
Published date 18 August 2015

http://www.aimspress.com/

Research article

Voltage biased Varistor-Transistor Hybrid Devices: Properties and Applications

Raghvendra K. Pandey [1,*], William A. Stapleton [1], Mohammad Shamsuzzoha [2], and Ivan Sutanto [1]

[1] Ingram School of Engineering, Texas State University, San Marcos, TX 78666, USA
[2] School of Mines and Energy Development, the University of Alabama, Tuscaloosa, AL35487, USA

* **Correspondence**: Email: rkpandey@att.net, or rkpandey@txstate.edu.

Abstract: The paper describes the properties and potential applications of a novel hybrid varistor device originating from biased voltage induced modified nonlinear current-voltage (I-V) characteristics. Single crystal of an oxide semiconductor in the family of iron-titanates with the chemical formula of Fe_2TiO_5 (pseudobrookite) has been used as substrate for the varistor. The modifications of the varistor characteristics are achieved by superimposition of a bias voltage in the current path of the varistor. These altered I-V characteristics, when analyzed, reveal the existence of embedded transistors coexisting with the varistor. These transistors exhibit mutual conductance, signal amplification and electronic switching which are the defining signatures of a typical transistor. The tuned varistors also acquire the properties of signal amplification and mutual conductance which expand the range of applications for a varistor beyond its traditional use as circuit protector. Both tuned varistors and the embedded transistors have attributes which make them suitable for many applications in electronics including at high temperatures and for radiation dominated environments such as space.

Keywords: voltage biased varistor; embedded transistors; hybrid devices; oxide semiconductor substrates

1. Introduction

The paper illustrates the coupled nature that exists between a varistor and a transistor and that forms the basis for the development of "varistor-transistor hybrid devices". These devices emerge when the nonlinear current-voltage characteristics (I-V) of a varistor diode is modified by the superimposition of a biasing voltage between the source (*S*) and drain (*D)* metallic contacts. The substrate material used for this research is pseudobrookite, F_2TiO_5, which is a nonconventional semiconductor and a prominent member of the family of iron-titanate oxide semiconductors. Single crystal samples of pseudobrookite (abbreviated as PsB) have been used to configure and analyze these devices. PsB along with another member of the iron-titanate family called ilmenite, $FeTiO_3$,have been studied for a long time for conversion of solar energy into clean hydrogen gas through photo catalysis reactions [1–3]. For these studies large single crystals of these two minerals were grown by the Czochralski technique and it was determined that their band gap, E_g, for PsB is 2.18 eV and for ilmenite is 2.34 eV [1].With the recent renewed interest in green energy the search for suitable materials for energy harvesting through photo catalytic process has intensified and many of them are processed by highly sophisticated techniques that are now available to us. Pseudobrookite plays an important role in search for alternative energy sources. Recently it has been identified that PsB nanoparticles could be good candidates as a new electrode material for Li-ion batteries [4].

Pseudobrookite crystallizes in orthorhombic structure with the lattice constants of a = 0.373, b = 0.979 and c = 0.993 nm having the space group of *Cmcm* [5].Based on high temperature studies of resistivity (ρ) and Seebeck coefficient (κ) it is found that PsB is a n-type semiconductor material with the band gap of 2.77 eV [6]. This measured value for the band gap is higher than the literature value of 2.18 eV reported for bulk pseudobrookite crystal [1]. This level of discrepancy in the values of the bandgap is not uncommon because it depends on the experimental methods used for its determination. Furthermore, for oxides it is also known that thermal treatments such as sintering and annealing in different environments can induce changes in such properties as resistivity, semiconducting nature (n-type or p-type), and bandgap [7]. The electronic structures and optical properties of pseudobrookite have also been reported only recently [8]. PsB is seldom found in nature as a magnetic material. However, when doped with Mn^{3+} ions it becomes a room temperature ferrimagnetic material exhibiting a well-developed hysteresis loop while still retaining its semiconducting nature. Mn-PsB ceramic appears to be an excellent material for the development of varistor based transistor.

2. Material and Method

Single crystal samples of pseudobrookite for this research were grown using the high temperature solution growth method (HTSG)for which the charge consisted of high purity grade pseudobrookite powder (acquired from Alfa Aesar) that was dissolved in a flux of $PbO.V_2O_5$.at about 1350 °C and recrystallized by very slow cooling between 1340 and 850 °C. The details of the crystal growth experiments varied only nominally from those reported in literature [9,10]. A large number of very shiny black platelets varying in sizes were harvested by dissolving the solidified flux in 25% nitric acid. A few of them were relatively large having the dimensions of 8–10 mm long × 1–1.5 mm thick × 2–3mm wide. They were characterized for crystal structure by X-ray diffraction (XRD) and

for elemental analysis and general surface morphology by energy dispersed X-ray diffraction (EDAX) methods. A few of the platelets with good surface uniformity were selected for different experiments. First they were annealed at about 1100 °C for 2–3 min a flowing argon environment to relieve thermal stress and to minimize their insulating nature so that they could acquire resistivity in the range suitable for producing currents above noise levels. Then they were polished to a high shine for making electrical contacts for the determination of the current-voltage characteristics. Only those samples were selected for XRD, EDAX and electrical measurements that were found to be free of surface irregularities and micro cracks.

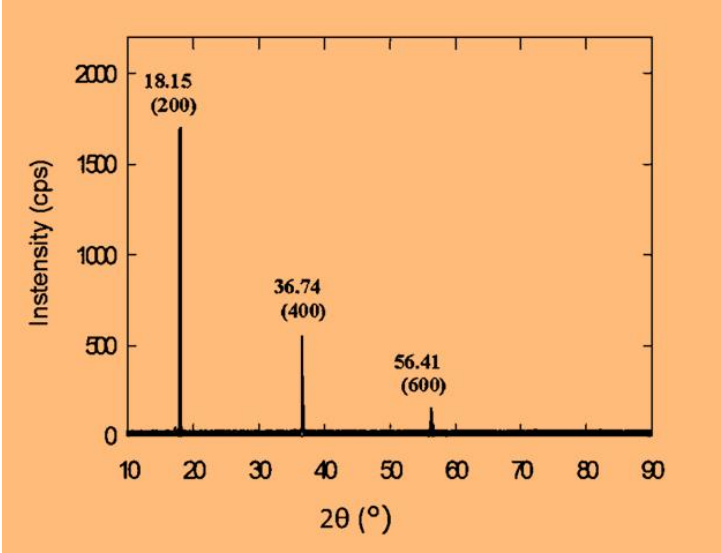

Figure 1. Intensity vs. 2θ plot of single crystal F2TiO5. Reproduced with minor modifications by permission from IEEE under license number: 3352730845893 [11].

Figure 1 shows the intensity vs. 2θ plot for PsB platelets. The *X-ray* diffraction analysis was carried out using a Bede D1 X-ray diffractometer which is capable of producing diffraction patterns with a high degree of resolution for determining the crystallographic orientations [11]. The samples were irradiated with CuKα radiation having the wavelength of 0.15418 nm. From Figure 1 we find that (h00) planes dominate and planes with non-(h00) orientation are not at all present in the sample. From this we conclude that (100) is the preferred growth plane for pseudobrookite crystallites.

Electron diffraction patterns of PsB single crystals were obtained using a 200 keV Hitachi H-8000 Transmission Electron Microscope. The bright field micrograph is shown in Figure 2(a) and the corresponding diffraction pattern in Figure 2(b). From the micrograph of Figure 2(a) we infer that the sample consists of two or three closely stacked planes having the common orientation of (100). This observation is supported by the indexed diffraction pattern of Figure 2(b) where we find that the common (100) planes are slightly mis-oriented by approximately 5.5 degrees. The electron beam pattern was obtained with the beam normal to the (100) plane [10].

The elemental analysis for the PsB crystals was determined by energy dispersed x-ray analysis (EDAX). Three different samples were selected for elemental analysis and ten randomly selected spots were analyzed. The results varied between 1–3% from sample to sample. The mean for iron and titanium were used as their respective values for the pseudobrookite crystal. For oxygen

concentration the sum of iron and titanium concentrations was subtracted from the nominal composition obtained from the chemical formula of $FeTi_2O_5$.The nominal concentrations of elements in pseudobrookite crystal according to the formula of $FeTi_2O_5$ should be in atomic %: Fe = 12.5%, Ti = 25% and O_2 = 62.5 %.It was found that iron and titanium were in excess by 3.45 and 3.76 atomic percent, respectively, whereas oxygen was deficient by 7.22 atomic percent compared to their nominal values. It is well known that EDAX is not a suitable method to determine the oxygen concentration correctly. Therefore the value given here for O_2 concentration in PsB crystal should be considered just an estimate and not exact.

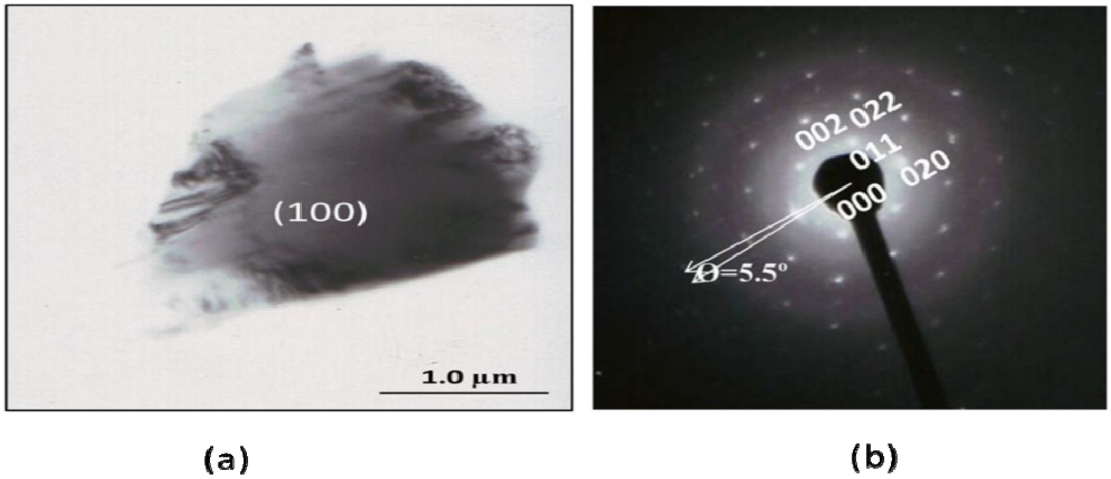

Figure 2. (a) TEM image of two or three rectangular shaped Fe_2TiO_5 (PsB) crystals that are closely stacked along the (100) common plane; and (b) Electron diffraction pattern taken with electron beam parallel to the [100] direction of the crystallites shown in (a). Here θ = 5.5° represents the angular misalignment between the stacked planes. Reproduced under license number 3600351213926 of Springer [10].

Apart from being a good wide bandgap and an n-type semiconductor material PsB is also a very good radiation hardened (radhard*)* material. The nonlinear I-V behavior of single crystal PsB shows remarkable immunity to irradiation, in particular to neutron and Fe-heavy ions. Samples were subjected to neutron stream of 73 MeV energy with a dose of 2.1×10^9 neutrons per cm^2 after which the output current remained virtually unaltered. A similar result was found when the samples were subjected to Fe-heavy ions with energy of 307 MeV/nucleon at dose of 3,000 rad [12]. We presume that the excellent radiation immunity of PsB makes it a potentially good candidate for developing devices suitable for space electronics.

3. Results and Discussion

Metallization: For electrical characterization a few polished and argon annealed samples were selected. Silver contacts spaced a few mm apart from each other were made on the top flat surface of the rectangular samples using high grade conductive epoxy. The circular contacts had a diameter of less than 0.5 mm. After air drying they were cured at about 250 °C in an oven for a few hours which

produced bright metallic silver contacts. Two sets of samples were prepared with silver dots; one with 4 dots spaced about 1mm apart and the other with just two dots, also about 1 mm apart. Completely linear I-V curves were obtained with all the samples with 4 points, whereas the samples with 2 point contacts produced nonlinear I-V plots with well-defined features. This suggested the possible formation of Schottky barriers at the interface of the metallic contact and the n-type substrate. This assumption can be validated based on capacitance vs. voltage (C-V) studies that Schottky barriers indeed form at the interface of silver and iron titanate substrate [13].In view of these observations we can assume that the rectifying nature of the 2-point I-V measurements using PsB samples have their origin in the potential barriers existing between the metallic silver contacts and the substrate. Migration of electrons from metal to semiconductor substrate overcoming the potential barrier is the physical basis for Schottky diodes. It is to be appreciated that varistors are also examples of Schottky diodes built on oxide semiconductor platforms. In fact the bipolarity of the varistor I-V, which we will encounter in subsequent sections, can be explained on the basis of the model which assumes that a varistor diode is equivalent to two Schottky diodes in back to back configuration with opposing polarities.

Device I: Unbiased Varistor and its voltage dependent resistor (VDR)

For I-V measurements a semiconductor parametric analyzer (Model HP-4145 B of Hewlett Packard, Palo Alto, CA, USA) was used. The samples were securely mounted on the test fixture using fine silver wires. The experimental set up was configured to minimize the leakage current. Additionally all measurements were done keeping the samples in complete darkness by closing the test box and covering it with a black piece of cloth. This prevented any interference from the surrounding light sources. The measurements were done by subjecting the samples to driving potentials by sweeping it continuously between the limits of ±7V. A large number of data points at close intervals were collected for analysis in each experiment.

For I-V measurements a standard circuit commonly used for the determination of I-V characteristics of an n-p-n bipolar junction transistor (BJT) was used [14]. It is shown in Figure 3.

The circuit configuration adheres to the Kirchhoff's current law according to which:

$$|I_d| \approx |I_s| + |I_b| \quad (1)$$

where I_d is the drain current, I_s the source current and I_b the bias current.

A cursory inspection of Figure 3 reveals that the superimposition of the bias current (I_b) at B results in the origin of three interconnected varistors identified here as: S-D, S-B and B-S, respectively. This simple electronic manipulation results in a platform for "varistor-transistor hybrid device (VTH)" having the potential for number of practical applications. The block diagram of Figure 4 serves as the roadmap representing the sequence that follows resulting in the existence of a VTH device. In the absence of the bias current the device reduces simply to a two terminal varistor diode.

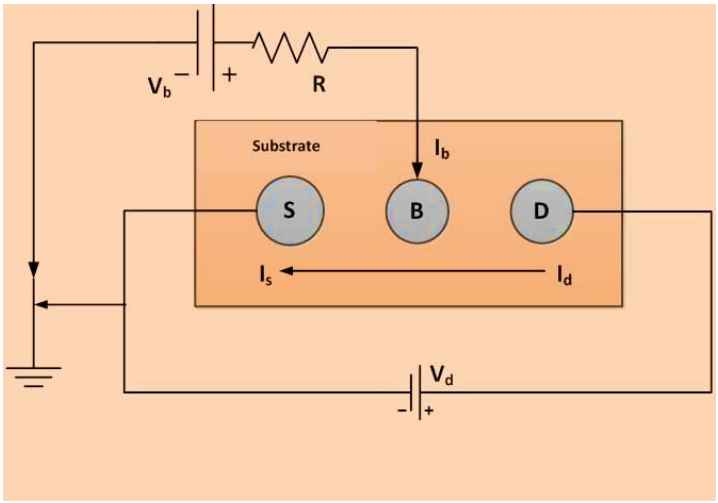

Figure 3. Standard circuit configuration for I-V determination. Here S, B and D are source, bias and drain contacts, respectively. Reproduced under IEEE Creative Common Attributes (CC-BY) agreement [14].

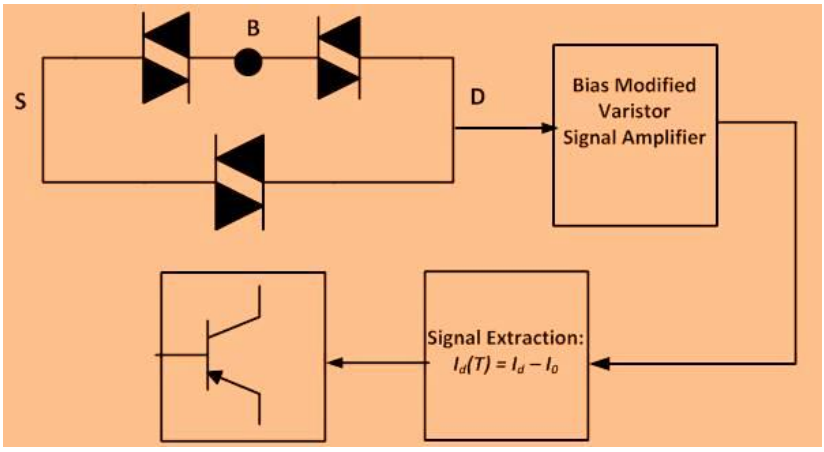

Figure 4. Block diagram showing three interconnected varistors, a varistor signal amplifier and a transistor. The labels S, B and D refer to the source, bias and drain terminals as shown in Figure 3. Reproduced under IEEE Creative Common Attributes (CC-BY) agreement [14].

First only the two terminal I-V characteristic of PsB varistor is determined which is shown in Figure 5 along with the associated resistance vs. voltage (R-V) mode of the varistor diode. The I-V plot shown in Figure 5 exhibits a few defining features that are uniquely inherent to a varistor diode. They are: (a) asymmetry with respect to (0,0) origin, (b) the existence of switching voltages, $\pm V_s$, identified in the figure by the two dashed parallel lines, (c) a passive range within the two dashed parallel lines in which the device has high impedance making the current close to zero, and (d) once the driving potential exceeds the threshold of switching voltages the varistor goes into low impedance state resulting in large currents to flow. The two switching voltages for the PsB varistor correspond to $+V_s$ at +1.2 V in the forward mode (for $+V_d$) and $-V_s$ at −0.8 V in the reverse mode ((for $-V_d$) of the device.

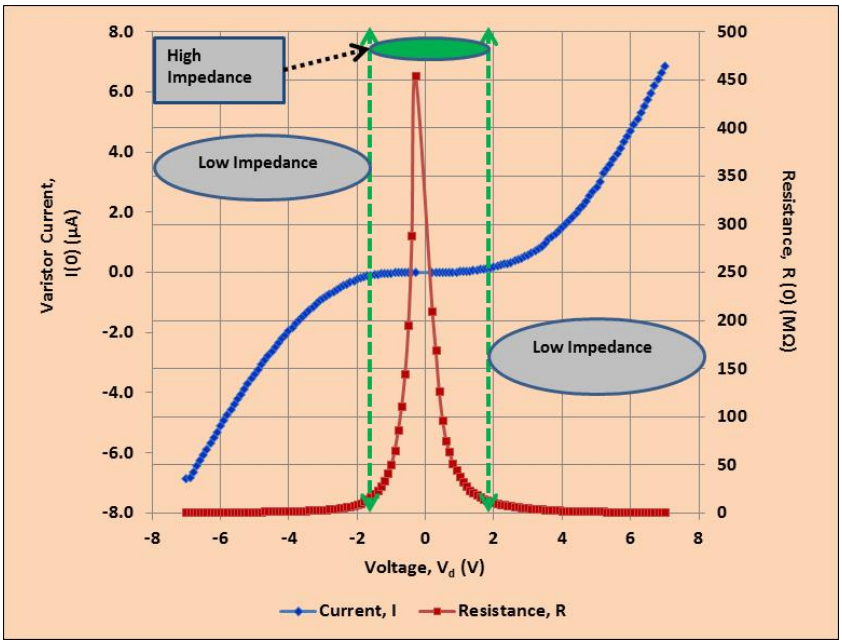

Figure 5.Current-voltage and resistance-voltage plots of a PsB varistor.

Conventional varistors are primarily used for protecting electrical circuits from sudden surges in line voltage caused by either severe thunderstorms and lightning or some technical failure at the power station. For this the varistors are connected in parallel to the load that needs to be protected and acts like a shunt to divert current from the protected device once the applied voltage surpasses the switching voltage of the varistor. Once the line voltage is restored, the varistor goes back to its dormant state after protecting the circuit components from being totally destroyed.

Apart from switching voltage the figure-of-merit of the device also plays an important role in real world applications of a varistor. The figure-of-merit for a varistor is also known as nonlinear coefficient (α). For PsB varistor it is found to be 2.78.In general, the current–voltage relationship for a varistor is given by an empirical formula of the type

$$I = cV^{\alpha} \qquad (2)$$

where c is a constant.

From the *R-V* plot of the varistor we can see that the resistance peaks at about $V \approx -0.3$ *V*. In this mode the varistor is called "voltage dependent resistor" or simply *VDR*. *VDRs* are also widely used devices since it allows for the precise output of resistance for a slight change in input voltage. For example, we find from the R-V plot of Figure 5 that the resistance changes by approximately 444 MΩ between its peak value at V = −0.3V and at V = +2 V which equates to a change of approximately 193 kΩ per mV. Such a large response is impressive suggesting one could build a very sensitive *VDR* device using PsB single crystal substrate. Once resistance reaches its peak value it decreases rapidly following the relationship

$$R = bV^{-\beta} \qquad (3)$$

where b is a constant and β the nonlinear coefficient (NLC) of *VDR*. We evaluate β to be −1.73 for the PsB *VDR* device.

The relationship between the two nonlinear coefficients, α and β, can be readily found by simple manipulation of equations (2) and (3) which yields:

$$-\beta = (1-\alpha). \qquad (4)$$

At this point it may be warranted to examine the cause for the emergence of a varistor like effect in a single crystal substrate. Normally we find varistor effects in a metal oxide ceramic semiconductor such as zinc oxide, ZnO. From well-established theoretical models we know that the current transport in a typical polycrystalline varistor takes place by a process known as G-GB-G (grain-grain boundary-grain) mechanism enabling the current-voltage characteristics to be nonlinear which is the hall mark of a varistor. Since single crysals do not have grain boundariesthere must be another mechanism that would contribute to the varistor effect like we find in PsB single crystal. A macroscopic model, called metal oxide-insulator-metal oxide (mo-i-mo) model, has been proposed to explain the existence of varistor like I-V in single crystals of ZnO. According to this model intermediate insulating layers are supposed to be the origin for the nonlinear charcteristics of the ZnO varistor. It has been shown experimentally that these insulating layers are sandwiched between the single cystals planes of ZnO [15].We reported earlier in this paper that the PsB single crystals were grown by using a flux consisting of PbOand V_2O_5 metal oxides.It is conceivable that our signle crystal substratesmight also consist of insulating flux layerssandwiched between its crystal planes which can facilitate the varistor like I-V characteristics to emerge.

Device II. Varistors with bias voltage superimposed

The nonlinear I-V characteristics of a varistor can be significantly modified by superimposing a bias potential between the source and drain terminals as shown in Figure 3 For all 3-point measurements the samples were biased by voltages (V_b) varying between ± 7 *V*. A few examples of modified I-V plots are shown in Figure 6.We can make some interesting observations the way the sign of the applied bias plays an important role in increasing the output current or decreasing it with respect to the original unbiased current.

In Figure 6 we find that when positive bias potentials are applied the output current is smaller than the original current whereas it is larger for negative bias potentials. The reason for such an influence on the varistor current can be attributed to the relative changes in the heights of the original potential barrier of the unbiased varistor when a bias voltage of certain magnitude and polarity is applied. It appears that when a positive bias is applied the barrier height increases diminishing the number of electrons with sufficient energy to overcome the new potential height. This results in smaller output currents than when the device was in its unbiased state. Exactly the opposite happens when a negative bias is applied. As its consequence the output current increases proportionately to the negative bias voltage applied. We will see in the subsequent sections how the sign of the bias potential plays an important role with respect to the properties of the embedded transistors. Also the application of a negative bias results in large signal amplification making the device more interesting for applications.

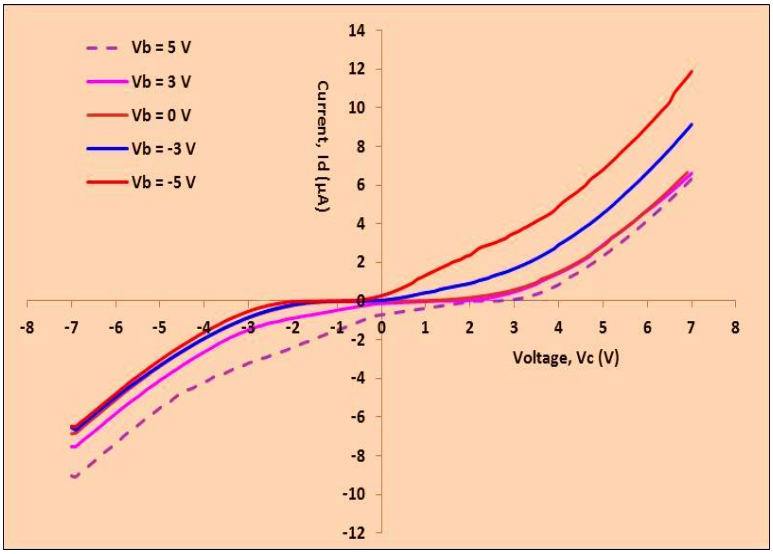

Figure 6. Current-voltage plots for a biased varistor for bias voltages, V_b = 0, ±3V, and ±6 V.

We can readily infer from Figure 6 that the negatively biased varistor becomes a signal amplifier and should be capable of boosting currents to meet the needs of many applications. This provides a straight forward and uncomplicated way to produce useful signal boosters. We can define the signal amplification as:

$$S(A) = \left[\frac{Current\ at\ V_b \geq 0}{Current\ at\ V_b = 0} \times 100\right]\% \qquad (5)$$

The maximum current amplification of almost 235 % can be achieved by this device under the conditions of drain voltage, V_d = +6V and bias potential, V_b = −6V. While the varistor assumes the quality of becoming a signal amplifier when negatively biased it becomes less efficient as a circuit protector. From Table I we find that its nonlinear coefficient, α, reduces from its peak value of 2.78 at zero bias to just about 0.78 at the bias potential of −6 V which amounts to a loss of about 72 % in its device efficiency making the varistor useless for circuit protection.

Table I. Biasing voltage, nonlinear coefficient, NLC (α) and its percentage change.

Bias Potential (V_b)	Varistor NLC, α	Normalized NLC (%)
0	2.78	100
−1	2.08	74.82
−2	1.65	59.35
−3	1.35	48.56
−4	1.12	40/29
−5	0.95	34.17
−6	0.78	28.06

Another remarkable feature of a biased varistor is that transistors can be produced by using some simple manipulations to determine the contributions made by bias potentials to the net output

currents. Normally they remain buried in I-V characteristics of the biased varistor until the transistor currents are filtered out for each biasing voltages. We can easily visualize that the modified varistor's net output current, I_d, consists of two components which are: (1) the original 2-terminal varistor current,I_0, when there is no bias present and (2) I_d (T) which is the contribution made by the bias potential to the original current I_0.In other words:

$$I_d = I_d(T) \pm I_0 \qquad (6)$$

The two currents, I_0 and I_d, are experimentally determined but the third current, I_d(T) can be filtered out from equation (6) using a simple subtraction step:

$$I_d(T) = I_d \pm I_0 \qquad (7)$$

The sign of I_d will obviously be dependent upon the relative magnitudes to the drain and bias currents. We can consider the two possible cases.
Case I: When $I_d > I_0$, then

$$+I_d(T) = I_d - I_0 \quad \text{for positive drain potentials, } +V_d \quad (8)$$

$$-I_d(T) = -I_0 - (-I_d) \quad \text{for negative drain potentials, } -V_d \quad (9)$$

Case II: When $I_d<I_0$, then

$$+I_d(T) = I_0 - I_d \quad \text{for positive drain potentials, } +V_d \quad (10)$$

$$-I_d(T) = -I_d - (-I_0) \quad \text{for negative drain potentials, } -V_d \quad (11)$$

Device III: Embedded transistor in a negatively biased varistor

From Figure 6 we find that this device is to be treated as Case I for which equations (8) and (9) apply. On completing the subtraction steps we obtain current-voltage characteristics for this transistor which is shown in Figure 7. We notice here that the transistor like I-V curves is present for both the positive and negative values of the driving potentials, V_d. The I-V curves are well pronounced and distinguishable from each other for the forward mode of the device enabling the transistor to be a good signal amplifier. The situation is exactly opposite for I-V plots in the reverse mode of the device. Here they are crowded and barely separable from each other.

In this mode we also observe that the transition of signals from positive to negative values takes place through the (0,0) origin enabling the transistor to acquire the property of electronic switching. Electronic switching along with capacity to amplify currents are the two defining properties of a transistor. The current amplification of approximately 2200% is achieved with V_d = +6 V and V_b = −6V. This level of signal amplification is impressive making the transistor comparable in performance to the conventional silicon based bipolar junction transistors (BJT). It is also interesting to note that this transistor is capable of amplifying currents almost ten times more strongly than the varistor from which it originates. Besides signal amplification and electronic switching, transconductance is another unique property of a transistor and is a key factor in designing current or voltage sources. The concept of transconductance is historically associated with vacuum tubes which predated the transistor era. Transconductance is also referred to as "mutual conductance" or "transfer function" and is assigned the symbol of G_m in literature. We can define mutual conductance with the

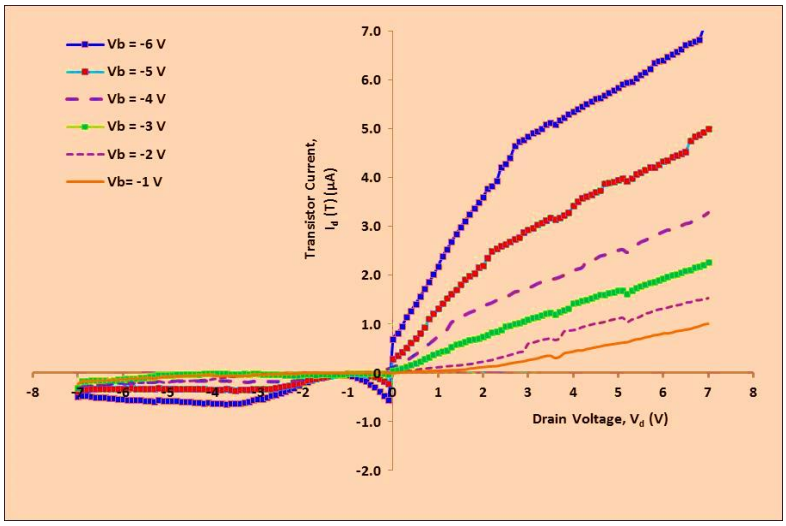

Figure 7. **Id(T) −V plots of a transistor with varying negative bias voltages, Vb.**

help of equation (12) which states that:

$$G_m(V_b) = \frac{transistor\ current}{bias\ voltage} = \frac{I_d(T)}{V_b} \approx \left(\frac{\Delta I_d\,(T)}{\Delta V_b}\right) (12)$$

Obviously the resistance associated with the mutual conductance is mutual resistance, R_m (= G_m^{-1}). The rule of thumb being that when G_m is large the device is good for current amplification and current source; whereas when it is small (high R_m) it is good for voltage amplification and voltage source. Using equation (12) we find with reference to Figure 7 that the transistor $G_m \approx$ 1.27 μS with V_d = +6V. Similarly we can calculate this parameter also for the biased varistor which we determine to be 1.06 μS for the identical condition of V_d = +6 V. We infer from these parameters that both the biased varistor and its embedded transistors are highly resistive devices having their respective mutual resistances in the MΩ range. The practical ramifications of these parameters are given in Table II.

Device IV. Embedded transistor in a positively biased varistor

Once the embedded transistor currents are extracted from the biased varistor currents using equations (10) and (11) we get transistor I-V curves which are plotted in Figure 8. Here each curve in the reverse mode of the device is well defined and amplification between each of them is large compared to the curves shown in the forward mode.

The picture here is exactly opposite to the one we encountered in Figure 7. Each curve for drain voltages varying between $0 < V_d < -7$V saturates after reaching its maximum value and remains saturated throughout. This is in contrast to the other condition when applied bias potentials were negative in sign. There the currents never saturated for any value of the bias potential suggesting that more and more electrons were still migrating to the conduction band and did not reach the state of equilibrium. Also from Figure 7 we infer the switching from negative current to positive current occurs through the origin of the two axes.

Table II. Selected device parameters and their applications.

Devices	Properties	Applications
Unbiased PsB Varistor		
(a) Current –Voltage Mode Nonlinear coefficient, NLC (α) Switching Voltage, $+V_s$	2.78 +1.2 V	μ-electronics circuit protection
(b) Resistance-Voltage Mode Nonlinear coefficient, NLC (β)	−1.73	Voltage Dependent Resistor (VDR)
Biased PsB Varistor with negative V_b at constant V_d = +6 V		
Maximum signal amplification Mutual conductance, G_m	≈ 235 % 1.06 μS	Simple current amplifier Current controlled voltage source, CCVS
Biased PsB Varistor with positive V_b at constant V_d = −6V		
Maximum signal amplification Mutual conductance, G_m	≈ 165 % 0.678 μS	Simple current amplifier Current controlled voltage source, CCVS
Embedded PsB Transistor with negative V_b at constant V_d = +6V		
Maximum signal amplification Mutual conductance, G_m	≈ 2200 % 1.27 μS	Strong current amplifier Current controlled voltage source, CCVS
Embedded PsB Transistor with positive V_b at constant V_d = −6 V		
Maximum signal amplification Mutual conductance, G_m	≈ 6000 % 0.774 μS	Strong current amplifier Current controlled voltage source, CCVS
Embedded MnPsB Transistor with negative V_b at constant V_d = +5V		
Maximum Signal Amplification Mutual conductance, G_m	≈ 500 % 0.252 mS	Current Amplifier Voltage controlled current source, VCCS.
Frequency response of PsB devices Experimental conditions fixed at V_b = 4 V and V_d = 5 Vpp		
(a) Varistor	Current peaks at 25 kHz	Acoustic amplifier Low pass filter with bandwidth of 135 kHz
(b) Embedded Transistor	Very small current Resonance peak around 125 kHz	Low pass filter with bandwidth of just about 2.5 kHz.

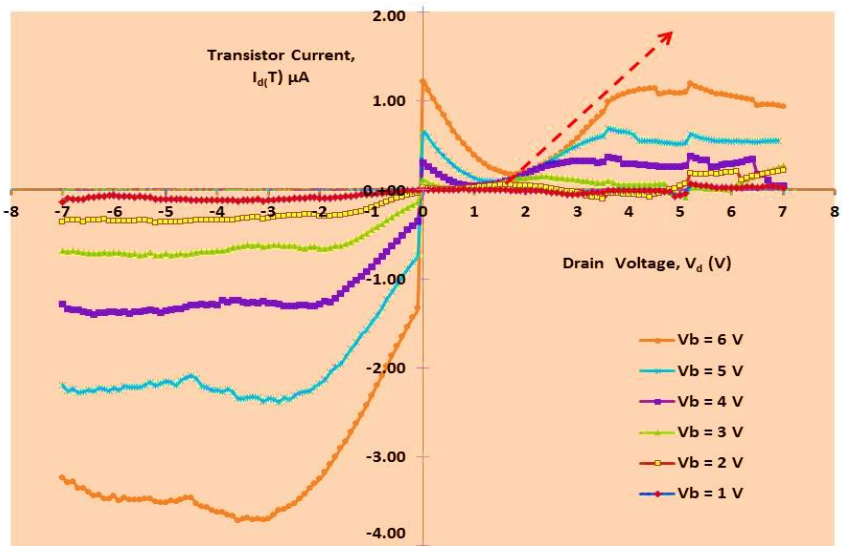

Figure 8. Id(T) −V plots of a transistor with varying positive bias voltages.

The maximum level of signal amplification for this transistor reaches a robust value of approximately 6000%. Both embedded transistors, one biased with negative potential and the other biased with positive potentials can compete well with conventional transistors (BJT) and have the potential to impact positively transistor technology. Their simplicity of fabrication on rugged and polycrystalline ceramic substrates that can withstand high temperature and irradiation are additional advantages in their favor. Using the definition described by equation (12) the value for its transconductance (G_m) for positively biased transistor is found to be 0.774 µS with drain potential, V_d = –6V. Compared to the device biased with negative potentials (Figure 7) the transistor biased with positive potentials is approximately 60% more conductive having as well the signal amplifying potential greater by a factor of 3.

In spite of the impressive signal amplifying property the single crystal based transistors have the drawback of producing output currents in low µA regime because of its inherently high resistive nature. This makes the signals susceptible to superimposed electronic noises. This drawback can be overcome by doping PsB with suitable elements that can reduce its resistance sufficiently to produce output currents in mA range. This we achieved when we produced a ceramic with the configuration of 0.55 PsB-0.45 Mn_2O_3. The samples were pressed as small cylindrical pellets following the processing steps as described in reference [6]. From EDAX analysis it was found that in these samples iron was deficient by 9.1%, titanium by 4.36 %, manganese by 7.05 % whereas rich in oxygen by 6.36% compared to their theoretical values calculated from the chemical formula of $0.55F_2TiO_5$-0.45 Mn_2O_3. These values represent the mean value for each element obtained by using the procedure described earlier. We believe that Mn^{+3}ions occupy the Fe^{+2} sites in the ceramic samples. Mn-doping enhances not only the electrical conductivity of pseudobrookite rather it also makes it strongly ferromagnetic [6].This level of discrepancy between the theoretical values and experimental values are common for oxides. The MnPsB ceramic is not only more conductive than PsB but also it is also strongly magnetic at room temperature making it suitable for producing magnetic transistors and sensors [6].

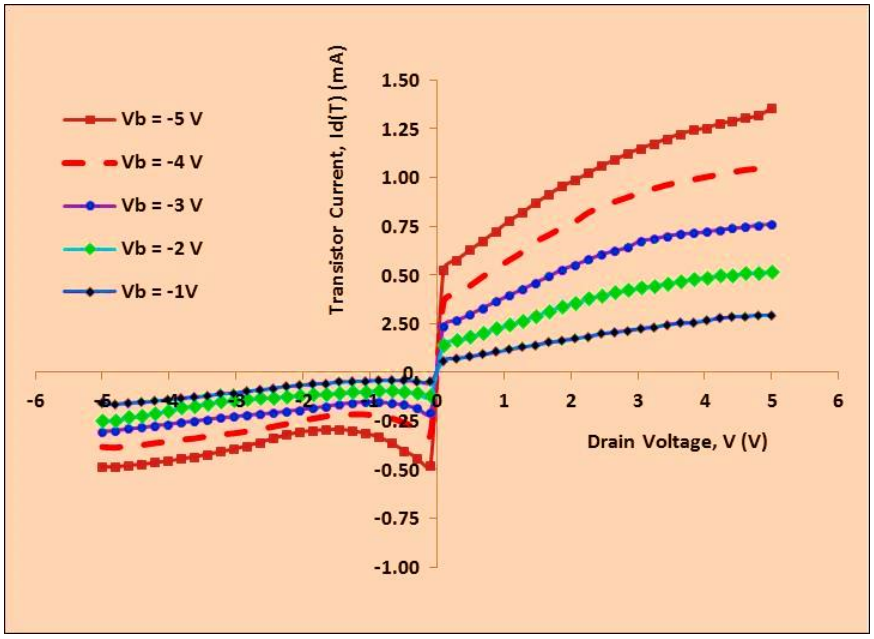

Figure 9. Id(T)-V plots of a MnPsB ceramic transistor with negative bias voltages.

The transistor current-voltage plots for MnPsB ceramic sample is shown in Figure 9. We clearly see from this that the output currents are in mA range and each I-V plot tending to saturate making the transistor suitable for general purpose applications. It is capable of current amplification as a good transistor reaching the value of almost 500% with V_d = +5 V and V_b = −5 V. The value of its transconductance (G_m) is found to be equal to 0.252 mS amounting to a value of 3.97 kΩ. From these parameters we infer that the relatively high value of transconductance of MnPsB ceramic transistors compared to their counterparts based on single crystal PsB substrates makes these devices more suitable for many applications where a large current output is a requirement. On the other hand its current amplification capability is much smaller than that of the PsB transistors still it remains at a level which is comparable to the values found for conventional transistors.

Frequency Response of Devices

The response of the positively biased varistor to in the frequency range of 100 Hz to 1 MHz was also studied. The frequency was changed and the corresponding output currents monitored.

From varistor response the contribution for the embedded transistor were extracted following the standard procedure already discussed. The frequency dependent output currents for both varistor and transistor are shown in Figure 10. Here the frequency response of the varistor is plotted for two conditions: (a) first when the device is unbiased and drain potential is at 5 Vpp; and (b) when a bias of +3 V is applied while still keeping the drain voltage constant at 5 Vpp. We notice here that the varistor current increases rapidly for both cases with frequency reaching its peak value at 25 kHz which is slightly above the outermost range of 20 kHz that a human being is capable of hearing. Nevertheless this varistor is suitable for developing audio amplifiers that can find many practical applications. The varistor can also be used as a low pass filter with bandwidth of 135 kHz. The blue curve represents the frequency dependence of the transistor with bias voltage being +3 V and drain voltage at 5 Vpp. Obviously the magnitude of the output current is substantially smaller than for the

parent varistor. Also we notice that it does it does not show any presence of a strong resonance peak like the varistor. However a very small peak can be identified around 125 kHz which is not distinguishable at the scale used in the figure. This device also acts like a low pass filter but with a bandwidth of only 2.5 kHz. The poor frequency response of the transistor mode limits its use in technology requiring a large bandwidth except perhaps in power electronics where a large bandwidth is not a requirement.

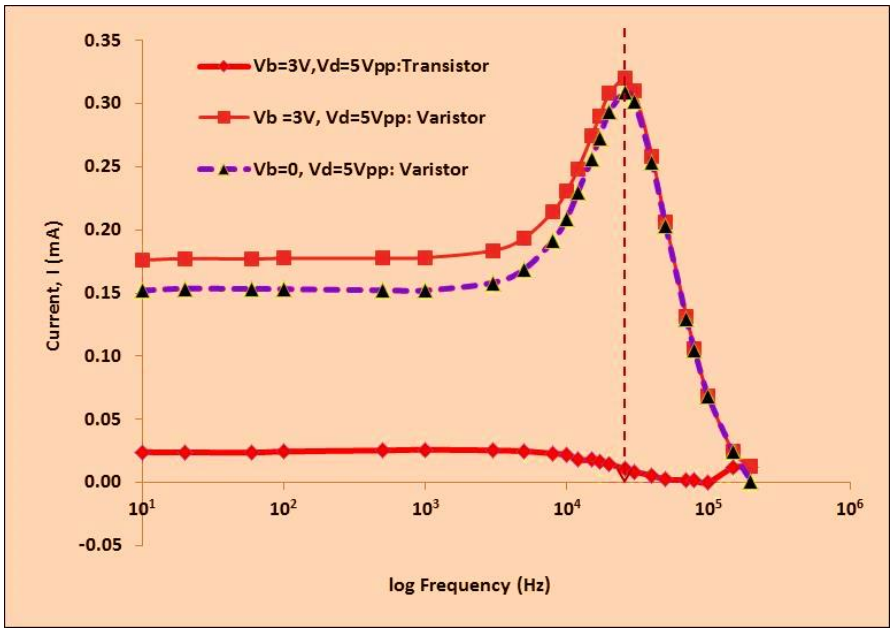

Figure 10. Frequency dependence of varistor and transistor currents based on PsB single crystals.

4. Conclusion

The paper describes how the current-voltage characteristics of a two terminal varistor can be tuned (or, modified) by the application of a superimposed bias voltage with the consequence of the emergence of new class of hybrid device consisting of a varistor and an embedded transistor.

The focus of the studies has been on the devices based on single crystal of pseudobrookite, Fe_2TiO_5, which is a member of the family of iron titanate wide bandgap oxide semiconductors. It is an n-type semiconductor with the bandgap of approximately 2.77 eV. For comparison sake we include here the bias potential induced transistors based on ceramic substrates of Mn-doped PsB where Mn is present at the level of 45 atomic %. The output currents of the MnPsB transistors are robust and are in mA range as compared to μA range of single crystal PsB transistors making it less susceptible to superimposition of electronic noises. Two types of embedded transistors based on PsB single crystal are described in this paper; one when the applied bias potential is positive and the other when it is negative. We find that the application of superimposed potentials for opposite polarity effect the basic properties of the transistors and thus their applications. We summarize the results in Table II making it easier to compare these devices and their potential applications.

Traditionally varistors are used primarily as circuit protector elements. We show in this paper that by biasing them with a voltage we can enhance their scope of practical applications. For example,

when it is biased by a voltage the varistor becomes a simple signal amplifier as well as it assumes the capacity for transfer function (mutual conductance) just like a traditional transistor. But as a circuit protector it becomes less efficient. Varistors show interesting frequency response making them potential candidates for fabrication of low pass electronic filters with a bandwidth up to 135 kHz. The varistor current increases with increasing frequency peaking at about 25 kHz which opens the possibility of using these biased varistors as platforms for fabricating audio amplifiers. However the frequency response of the transistors is poor with the bandwidth of just about 2.5 kHz.

Based on experimental evidence it is shown that a strong coupled relationship exists between a varistor and a transistor. The bias voltage induced changes in the I-V characteristics of the varistor are found to be the home of embedded transistors which bear resemblance with the widely used conventional bipolar junction transistors, BJT. In fact these embedded transistors are analogous to a BJT but the similarity is superficial. The physical principles on which a varistor embedded transistor and a BJT are based are different from each other. The configuration shown in Figure 4 demonstrates clearly that these ceramic transistors are not based on the configuration of a BJT which can be either n-p-n or p-n-p. These transistors belong to a new class of transistors which can be produced on ceramic substrate of an oxide semiconductor. These hybrid devices could be fabricated on a single chip with dual functions of a varistor and a transistor. Since pseudobrookite is an excellent radhard material, remains a good n-type semiconductor up to 700 °C and consists of bio compatible materials like iron oxide and titanium oxide, it is conceivable that these devices could find their applications also in space electronics, at high temperature electronics, and bioelectronics apart from the other applications already discussed.

Acknowledgments

We acknowledge the support of the National Science Foundation *(NSF)*, Grant # ECCS-1025395. We also thank Professor Wim Geerts of the Department of Physics at Texas State University for allowing us the extensive use of the semiconductor parametric analyzer (HP-4145 B) in his laboratory which made this research possible.

Conflict of Interest

The authors declare no conflicts of interest in this paper.

Reference

1. Ginley D, Butler M (1977) The photoelectrolysis of water using iron titanate anodes. *J Appl Phys* 48: 2019.
2. Morison B, Baughman R, Ginley D, et al. (1978) The influence of crystal structure on the photoresponse of iron–titanium oxide electrodes. *J Appl Cryst* 11: 121–124.
3. Kazuka H, Kajimura M (2001) Sol-gel preparation and photoelectrochemical properties of Fe_2TiO_5 thin films. *J Sol Gel Sci Tech* 22: 125–132.
4. Min K, Park K, Lim A, et al. (2012) Synthesis of pseudobrookite-type Fe_2TiO_5 nanoparticles and their Li-ion electroactivity. *Ceram Int* 38: 6009–6013.

5. Pauling L (1930) The crystal structure of pseudobrookite, *Z. Krystallographie-Crystalline Materials* 73: 97.
6. Pandey R, Stapleton W, Sutanto I, et al. (2014) Processing properties of advanced ceramics and composites VI. *Ceram Transactions*, John Wiley and Sons; 249: 175.
7. Mizusaki J, Tabuchi J, Matsuura T, et al. (1989) Electrical conductivity and Seebeck coefficient of nonstoichiometric $La_{1-x}Sr_xCoO_{3-\delta}$. *J Electrochem Soc* 136: 2082–2088.
8. Jin L, Zhou C (2013) Electronic structures and optic properties of Fe_2TiO_5 using LSDA+*U* approach. *Prog Nat Sci Mater Int* 23: 413–419.
9. Garten G, Smith S, Wanklyn B (1972) Crystal growth from the flux systems $PbO \cdot V_2O_5$ and $Bi_2O_3 \cdot V_2O_5$. *J Cryst Growth* 13/14: 588–592.
10. Pandey R, Stapleton W, Sutanto I, et al. (2015) Voltage-Biased Magnetic Sensors Based on Tuned Varistors. *J Electron Mater* 44: 1100–1109.
11. Pandey R, Padmini P, Deravi L, et al. (2006) Magnetic-semiconductors in Fe-Ti-oxide series and their potential applications. *IEEE Proceedings of the 8th International Conference on Solid State and Integrated Circuit Technology* 2: 992.
12. Pandey R, Padmini P, Schad R, et al. (2009) Novel magnetic-semiconductors in modified iron titanates for radhard electronics. *J Electroceram* 22: 334–341.
13. Lohn C, Geerts W, O'Brien C, et al. (2008) Functionalized Nanoscale Materials, Devices and Systems. NATO Science for Peace and Security Series B: Physics and Biophysics, 419.
14. Pandey R, Stapleton W, Sutanto Iv (2015) Nature and characteristics of a voltage-biased varistor and its embedded transistor. *J Electron Dev Soc* 3: 276–284.
15. Schwing U, Hoffmann B (1980) ZnO single crystals with an intermediate layer of metal oxides—A macroscopic varistor model. *J Appl Phys* 51: 4558.

AIMS Press